EJN European Journal of Neuroscience

FENS Federation of European Neuroscience Societies

European Journal of Neuroscience, Vol. 44, pp. 2899–2908, 2016 doi:10.1111/ejn.13413

NEUROSYSTEMS

Intralaminar and tectal projections to the subthalamus in the rat

Takako Kita,[1] Naoki Shigematsu[2] and Hitoshi Kita[1]
[1]Department of Anatomy and Neurobiology, College of Medicine, The University of Tennessee Health Science Center, 855 Monroe Avenue, Memphis, TN 38163, USA
[2]Department of Anatomy and Neurobiology, Graduate School of Life Sciences, Kumamoto University, Kumamoto, Japan

Keywords: parafascicular nucleus, subthalamic nucleus, subthalamus, zona incerta

Edited by László Acsády
Received 25 July 2016, revised 19 September 2016, accepted 21 September 2016

Abstract

Projections from the posterior intralaminar thalamic nuclei and the superior colliculus (SC) to the subthalamic nucleus (STN) and the zona incerta (ZI) have been described in the primate and rodent. The aims of this study was to investigate several questions on these projections, using modern neurotracing techniques in rats, to advance our understanding of the role of STN and ZI. We examined whether projection patterns to the subthlamus can be used to identify homologues of the primate centromedian (CM) and the parafascicular nucleus (Pf) in the rodent, the topography of the projection including what percent of intralaminar neurons participate in the projections, and electron microscopic examination of intralaminar synaptic boutons in STN. The aim on the SC-subthalamic projection was to examine whether STN is the main target of the projection. This study revealed: (i) the areas similar to primate CM and Pf could be recognized in the rat; (ii) the Pf-like area sends a very heavy topographically organized projection to STN but very sparse projection to ZI, which suggested that Pf might control basal ganglia function through STN; (iii) the projection from the CM-like area to the subthalamus was very sparse; (iv) Pf boutons and randomly sampled asymmetrical synapses had similar distributions on the dendrites of STN neurons; and (v) the lateral part of the deep layers of SC sends a very heavy projection to ZI and moderate to sparse projection to limited parts of STN, suggesting that SC is involved in a limited control of basal ganglia function.

Introduction

The main nuclei in the subthalamus are the subthalamic nucleus (STN) and the zona incerta (ZI). STN is considered to be an input nucleus of the basal ganglia because it receives inputs from outside the basal ganglia and sends its outputs mainly to the nuclei within the basal ganglia (Kita, 1994). Glutamatergic inputs from the posterior intralaminar thalamic nuclei and the superior colliculus (SC) to the subthalamus have been described, in addition to well described cortical and pedunculopontine inputs (Sugimoto *et al.*, 1983; Groenewegen & Berendse, 1990; Mouroux & Feger, 1993; Tokuno *et al.*, 1994; Bevan & Bolam, 1995; Bevan *et al.*, 1995; Coizet *et al.*, 2009; Kita & Kita, 2011; Watson *et al.*, 2015). There are several issues regarding the intralaminar and SC projections to STN and ZI that need to be clarified to advance our understanding of the role of these nuclei. The present study examined the following anatomical questions using sensitive Fluoro-Gold (FG) retrograde and lentivirus (LV) anterograde tracing methods.

The posterior intralaminar thalamic nuclei project to multiple basal ganglia nuclei including the striatum, the external segments of the globus pallidus, and the subtalamus (Groenewegen & Berendse, 1994; Bevan *et al.*, 1995; Deschenes *et al.*, 1996; Yasukawa *et al.*, 2004; Galvan & Smith, 2011). The posterior intralaminar thalamic nuclei in the primate and the feline consist of the centromedian (CM) and the parafascicular nucleus (Pf), which can be identified by differences in their histological features and in their projection sites (Kuhlenbeck, 1954; Albe-Fessard *et al.*, 1966; Sadikot *et al.*, 1992; Parent & Hazrati, 1995; Smith *et al.*, 2014). The posterior intralaminar nuclei send topographically organized heavy projections to the striatum. In the monkey, the medial two-thirds of CM projects to the sensorimotor territory, the anterior part of Pf to the limbic territory, and the caudal and the dorsolateral extension of Pf to the association territory of the striatum (Smith *et al.*, 2014). In the rodent, identifying CM and Pf by histological features is difficult, and the designation Pf has been used to cover both nuclei, although early researchers described two nuclei, and some studies on the Pf-striatal projections suggested that the CM equivalent exists in rodent Pf (Groenewegen & Berendse, 1994; Galvan & Smith, 2011). In order to avoid confusion, we will use the designation CM+Pf for the rat

Correspondence: Hitoshi Kita, as above.
E-mail: hkita@uthsc.edu

in this report. Deschenes *et al.* (1996) suggested that the ethmoid thalamic nucleus (Eth) be included in the posterior intralaminar nuclei based on the similarity of cellular morphology and the projection sites. Thus we examined whether newer histological methods and projection patterns to the subthalamus can be used to differentiate CM, Pf, and Eth in the rodent.

CM+Pf projections to the subthalamus were described in the monkey, cat, and the rat. However, the reports are inconsistent regarding the topographical organization of these projections. For instance, early studies in the monkey and the cat described CM+Pf projections to ZI, STN, and the lateral hypothalamic area (LHA; Sugimoto *et al.*, 1983; Royce & Mourey, 1985), while a more recent study in monkeys was unable to confirm any of these projections (Parent & Parent, 2005). Studies in the rat showed that Pf mainly projects to STN and has some projections to ZI and LHA (Sugimoto *et al.*, 1983; Mouroux & Feger, 1993; : Mouroux *et al.*, 1995; Groenewegen & Berendse, 1990; Bevan *et al.*, 1995). Thus it is unclear whether CM+Pf projections to the subthalamus control mainly basal ganglia functions through the STN and/or other functions through ZI and LHA. The reports are also unclear whether all parts of CM+Pf project to the nuclei in the subthalamus and what percent of CM+Pf neurons participate in the projections. We examined these issues using advanced neurotracing methods.

The pathways in the cortico-basal ganglia loops maintain a parallel functional topography, although functional territories in each nucleus have various degrees of overlap. For instance, monosynaptic cortico-striatal and cortico-STN projections have functional topographical organizations, and the topographical relations are maintained in subsequent polysynaptic pathways such as the cortico-striato-pallido-STN and the cortico-STN-pallidal pathways (Groenewegen & Berendse, 1990; Smith *et al.*, 2010; Kita *et al.*, 2014). It is unknown whether the CM+Pf projections to STN match the topographical organization formed by other afferents. As Bevan *et al.* (1995) discussed in detail, descriptions of the topography including the main site of origin in CM+Pf in the previous studies are inconsistent (Sugimoto *et al.*, 1983; Groenewegen & Berendse, 1994; Bevan *et al.*, 1995; Deschenes *et al.*, 1996). We have shown that cortical projections to the subthalamus form functional topography encompassing both STN and ZI (Kita *et al.*, 2014). Thus, we examined the possibility that a similar functional topography exists in CM+Pf projections to the subthalamus.

We found only one electron-microscopy study on the thalamo-STN projections. Bevan *et al.* (1995) reported that rat CM+Pf and cortical afferents formed synaptic boutons having similar morphological features and that CM+Pf synapses were found on slightly larger dendrites than cortical ones. We reexamined the distributions of synaptic sites by comparing them to our previous data on the distribution of the postsynaptic sites of randomly sampled asymmetrical synapses (Chang *et al.*, 1983).

The SC projection to ZI has been well documented (Roger & Cadusseau, 1985; Shammah-Lagnado *et al.*, 1985; Kolmac *et al.*, 1998; Tokuno *et al.*, 1994; Mitrofanis, 2005; Watson *et al.*, 2015). The main controversy regarding the tectal projection to the subthalamus is whether main projection sites include STN. Early studies reported that SC projects mainly to the ventral ZI (ZIv) and sparsely to STN (Roger & Cadusseau, 1985; Shammah-Lagnado *et al.*, 1985; Tokuno *et al.*, 1994; Kolmac *et al.*, 1998). However, recent studies reported a heavy projection that arises predominantly from the lateral SC deep layers and terminates preferentially in the rostral and dorsal sectors of the STN (Coizet *et al.*, 2009). A more recent study confirmed early studies that SC projects mainly to ZIv and minor to STN (Watson *et al.*, 2015). We have reexamined these questions.

Materials and methods

Animal preparation and brain sectioning

The present study used 31 male Sprague–Dawley rats (280–380 g, Charles River Laboratories, Wilmington, MA, USA). All procedures were approved by The University of Tennessee Health Science Center Animal Care and Use Committee (approval number 13-161.0-A) and were in compliance with the National Institutes of Health Guide for Care and Use of Laboratory Animals. To label neurons projecting to the subthalamus, the Fluoro-Gold (FG) retrograde labeling method was used. For anterograde labeling, we used lentiviruses (LV) VSVG.HIV.SIN.Synapsin.ChR2(H134R).EYFP.WP (Y483, Penn Vector core). We were familiar with this LV because we used the same virus in our physiological studies. For FG and LV injections, a glass micropipette was glued to the needle of a 10 μL Hamilton microsyringe, which was filled with 0.3% FG or viruses, 1×10^6 infectious particles/μL, in saline. Rats were anesthetized (i.p.) with a mixture of Ketamine (60 mg/Kg, Pfizer, Inc. New York City, NY, USA) and Xylazine (10 mg/Kg, Agri Lab. St. Joseph, MO, USA) and placed on a stereotaxic apparatus. A craniotomy over a target area was made for the penetration of the pipette. FG (0.1 μL) or LV (0.1 μL) was injected slowly (0.02 μL/min) by advancing the microsyringe plunger with an electric actuator.

Preparations for light microscopy

After 10 days for FG and 3 weeks for LV of survival, the rats were deeply anesthetized with a mixture of Ketamine (100 mg/Kg) and Xylazine (20 mg/Kg) and were perfused through the heart with 10–20 mL of isotonic saline followed by 200–300 mL of a fixative (mixture of 4% formaldehyde and 0.2% picric acid in a 0.12 M sodium phosphate buffer, pH 7.4). After perfusion, the brains were removed and postfixed overnight at 4 °C and then equilibrated in a 10% followed by a 30% sucrose phosphate buffer (pH 7.4). The brains were cut into 40 μm coronal sections on a freezing microtome. The serial sections were divided into 4–8 sets for different uses.

Immunohistochemistry for FG and EYFG

Immunostaining for FG and EYFP was performed for amplification and transmitted light microscopic visualization of FG-containing neurons and LV-infected axons and boutons. Sections were treated in the following order: (i) preincubated in PBS containing 0.5% non-fat dry milk and 0.2% Triton-X for 2–3 h; (ii) incubated overnight in PBS containing rabbit anti-FG serum (1 : 15 000, a gift from Dr H.T. Chang) or rabbit anti-EYFP (1 : 2000, Invitrogen, Cat# A-11122); (iii) rinsed four times with PBS and incubated in biotinylated anti-rabbit antibody (0.5 μg/mL) for 1.5 h; (iv) rinsed four times with PBS and incubated in an avidin-biotin-peroxidase complex (ABC, 1 : 100, Vector Laboratories) for 1.5 h; (v) rinsed four more times; and (vi) incubated in PBS containing 3,3′-diaminobenzidine (0.05%), NiCl (0.001%), and H_2O_2 (0.003%), which produced dark-blue staining of labeled neurons and axons.

Some of the sections stained for FG and EYFP were further processed for second immunostaining for the calcium binding protein parvalbumin (PV), transcription factor Forkhead box protein P2 (FoxP2), or neuron-specific nuclear protein (NeuN). STN contains abundant PV immunoreactive (PV+) axons and terminals. Thus PV staining delineates STN from surrounding structures (Fig. 1). The PV stained sections were also used for subdividing ZI into dorsal and ventral ZI (ZId and ZIv): the former is pale with scattered PV+

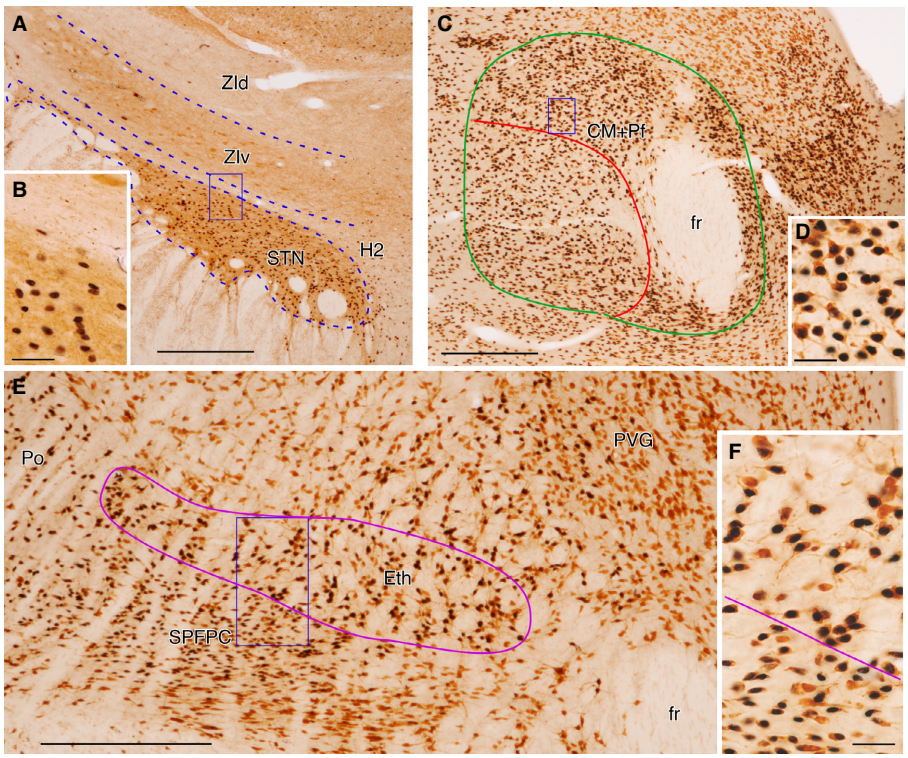

FIG. 1. (A) A section immunostained for PV (brown) and FoxP2 (stained nuclei black) shows that STN contains abundant PV+ axons and FoxP2+ neurons. LHA contains scattered FoxP2+ neurons, while H2 and ZI are free of FoxP2+ cells. ZIv contains more PV+ neurons and axons than ZId. (B) A higher magnification view of the boxed area in A. (C) A section immunostained for FoxP2 (stained nuclei black) and NeuN (brown) show that most of CM+Pf neurons are Foxp2+. The ventrolateral part of CM+Pf, marked by a red line, has a lower density of neurons compared to the dorsolateral and medial parts of CM+Pf. (D) A higher magnification view of the boxed area in C. (E) A section immunostained for FoxP2 and NeuN shows Eth with Foxp2+ neurons. (F) A higher magnification view of the boxed area in E. The scale bars in (A, C, and E) are 0.5 mm, and the scale bars in (B, D, and F) are 50 μm. [Color figure can be viewed at wileyonlinelibrary.com].

neurons, while the latter is darker due to abundant PV+ axons and terminals and numerous oval-shaped PV+ neurons. The Forel field H2 is a pale, narrow border area between STN and ZIv and contains small PV negative (PV−) neurons surrounded by axons. We also used FoxP2 staining to identify STN and CM+Pf as these nuclei in mice contain abundant FoxP2+ neurons (Campbell *et al.*, 2009; Reimers-Kipping *et al.*, 2011). The NeuN monoclonal antibody recognizes NeuN in most central nervous systems of vertebrates (information provided by Millipore) including the subthalamus, Pf, and SC (Celio and Heizmann, 1981; Kita & Kita, 2001). The sections were incubated overnight in PBS containing anti-PV monoclonal antibody (1 : 4000, Swant, PV235), anti-FoxP2 monoclonal antibody (1 : 2000, Millipore MABE415), or monoclonal antibody for NeuN (1 : 2000, Millipore MAB377), followed by biotinylated anti-mouse antibody (0.5 μg/mL, Vector Laboratories, BA-2000) for 1.5 h and avidin-biotin-peroxidase complex (ABC, 1 : 100, Vector Laboratories) for 1.5 h. Then, the peroxidase was revealed by incubating in PBS containing 3,3′-diaminobenzidine (0.05%) and H_2O_2 (0.003%). This reaction produced yellow-brown staining. After several rinses, immunostained sections were mounted on gelatin-coated slides, air-dried, dehydrated in graded alcohols to xylene, and coverslipped.

Light microscopic observation

The slides were observed under an Olympus microscope (Olympus BX50) with a drawing tube. Original drawings of the FG labeled neurons in the thalamus and SC and YGFP labeled terminal fields in the subthalamus were made under an ×40 objective, with one mark for every approximately five neurons or 10 boutons. Many landmarks such as blood vessels and fiber bundles were also drawn. Microscopic images were acquired by a digital camera (Nikon D70). Images were assembled in Adobe Photoshop (CS4) and Deneva Canvas-X, with adjustments for contrast, brightness, and color balance to obtain optimal visual reproduction of the data.

Preparations for electron microscopy

Glutaraldehyde (0.1%) was added to the fixative for the rats used for the electron microscopic (EM) observation of EYFP-labeled boutons, and the brains were cut into 50 μm thick horizontal sections on a Vibratome. The sections containing STN were equilibrated in 30% sucrose, freeze-thawed in liquid nitrogen, and then processed similarly to those described for light microscopy, with the exception that all the procedures were performed at 4 °C, and the sections were not treated with Triton X-100. After diaminobenzidine reaction, sections were postfixed with 1% osmium tetroxide, stained en bloc in 1.5% aqueous uranyl acetate, infiltrated with Epon-Araldite resin, mounted on Liquid Releasing Agent (Electron Microscopy Sciences, 70880) coated glass slides, and coverslipped. Areas of STN containing EYFP-labeled boutons were remounted on plastic blocks, and ultrathin (55–60 nm) sections were cut. The thin sections were examined and photomicrographed at 60 KV on a JEOL 1200 microscope and at 100 KV on a Hitachi H7500 microscope.

Results

Methods to identify STN, ZI, CM+Pf, and other areas

We identified the dorsal border of STN using PV and FoxP2 immunohistochemistry (Fig. 1A and B). The FoxP2 and PV staining also clearly revealed a thin extension of STN in the dorsolateral direction (Fig. 1A). We found that over 95% of rat STN neurons are FoxP2+ (Kita and Kita, unpublished data). ZI is free of FoxP2+ cells, and LHA contains scattered FoxP2+ neurons. The PV staining separates PV+ neuron and fiber-rich ZIv from PV-poor ZId.

The existence of a high population of FoxP2 neurons and high cell density distinguished CM+Pf from the surrounding areas (Fig. 1C and D). We estimated that over 90% of CM+Pf neurons were Foxp2+ (Kita and Kita, unpublished data). Figure 1C shows that the density of neurons in the ventrolateral part of CM+Pf is noticeably lower than the dorsolateral and medial parts of CM+Pf. The Eth contained neurons of similar size and shape as the FoxP2+ CM+Pf neurons and was located dorsal to the parvicellular part of the subparafascicular thalamic nucleus that contains small horizontally oriented FoxP2 neurons (Fig. 1E and F). FoxP2+ neurons were also found in the reticular area dorsal to Eth and the posterior thalamic nuclear group lateral to Eth. We drew the dorsal and lateral borders of Eth based on differences in the cell density. Because the dorsal and lateral borders were often could not be determined unequivocally, cell count analysis in Eth was not included.

Fluoro-Gold retrograde tracing

FG was injected to STN of eight rats. When FG injection covered the mid-rostrocaudal and mid-mediolateral parts of STN, numerous FG-labeled (FG+) neurons were observed in the dorsolateral part of CM+Pf (Figs 2A and 3). Eth also contained a large number of FG+ neurons (Fig. 2A). When FG injection site covered the medial part of STN and an adjacent part of LHA, numerous FG+ neurons were observed in the medial part of CM+Pf (Fig. 2B). In both the medial and lateral injection cases, only sparsely distributed FG+ neurons were observed in the ventrolateral part of CM+Pf. In all cases, sparsely distributed labeled neurons were also observed in the mediodorsal thalamic nucleus, the centrolateral thalamic nucleus, the posterior part of the anterior pretectal nucleus (APT), and the periventricular gray. FG+ neurons were also sparsely distributed in the posterior thalamic nuclear group, the deep layers of SC, and the central gray. These FG tracing results suggest that the posterior intralaminar nuclei, CM+Pf and Eth, are major origins of STN projections and that the anterior intralaminar nuclei, the midline thalamic nuclei, and SC projections to STN are minor. The percentage of FG+ neurons in heavily labeled areas of CM+Pf was estimated using cases of FG injection covering a large portion of STN and sections doubly immunostained for FG and NeuN (Fig. 3). Figure 3C shows a plotting of a section that resulted in the highest percentage, 31.8%, of all CM+PF neurons in this section. When only the dorsolateral area was counted, 52.1% were FG+ neurons.

FG injections confined to ZI were made in seven rats and resulted in a high concentration of FG+ neurons in the rostrolateral part of the deep layers of SC and the caudodorsal part of the APT. Many FG+ neurons were also distributed in the thalamic reticular area, the posterior thalamic nuclear group, the deep mesencephalic nucleus, the periventricular gray, the anterior part of the periaqueductal gray, and scattered FG+ neurons were present in the lateral habenular nucleus and Pf (Fig. 2C). These FG tracing results suggest that SC and the posterior part of the APT project heavily to ZI.

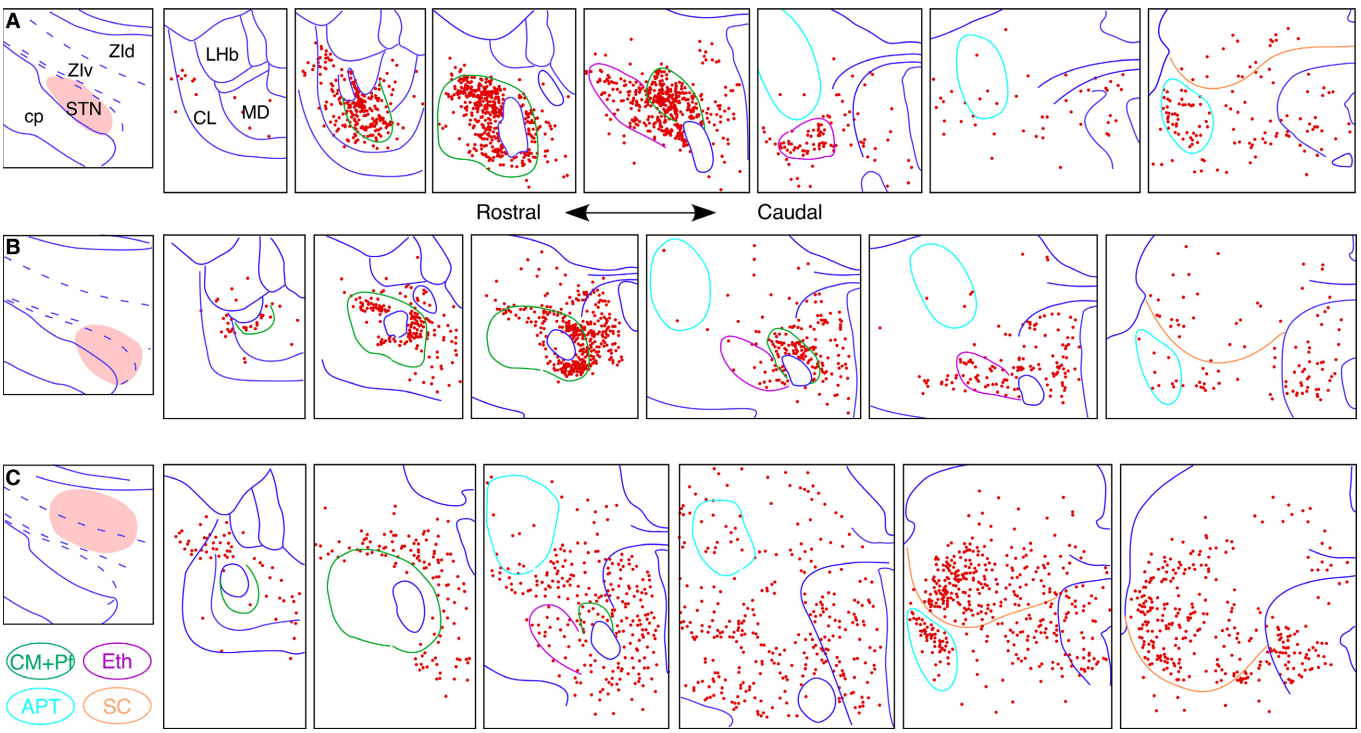

FIG. 2. Drawings of sections showing the distribution of FG+ neurons in the thalamus and dorsal midbrain after an FG injection into the STN (A and B) and ZI (C). [Color figure can be viewed at wileyonlinelibrary.com].

Lentiviruses anterograde tracing

Anterograde tracing experiments using LV were performed to substantiate the results of FG tracing experiments. LV injections in CM+Pf were performed in 10 rats. LV injections to the lateral part of CM+Pf resulted in heavy labeling of axons and terminals in the lateral and middle parts of STN and moderate labeling in the medial 1/3 of STN (Fig. 4A). These injections resulted in dense labeling in a large area of the striatum including the rostrodorsal and lateral sensorimotor territory and the middle association territory. In the cerebral cortex, moderate labeling was observed in the anterior part of the medial agranular cortex and in the lateral orbital cortex and very sparse labeling in the lateral agranular cortex and caudal part of the medial agranular cortices. LV injection in the medial part of CM+Pf resulted in heavily labeled axons and terminals in the medial 2/3 of STN (Fig. 4B). These injections resulted in dense labeling in the the accumbense, the ventral and medial limbic part of the striatum, moderate labeling in the middle association part of the striatum, and very sparse labeling in the medial agranular cortex and the insular cortex. In both cases, the Forel field H2 and LHA contained moderate densities of labeled terminals, and ZI contained very sparse labeling of terminals (Figs 4 and 5). LV injections that covered the rostral part of CM+Pf and the adjacent centrolateral thalamic nucleus resulted in moderate labeling in the rostrodorsal half of STN, and injections to the anterior intralaminar thalamic nuclei alone resulted in very sparse labeling of axons in STN and ZI (figures not shown).

The axons leaving CM+Pf traveled rostrally and entered the internal capsule. The collaterals of some ascending main axons descended through the internal capsule and entered STN from its rostral or ventral border, as shown previously by Deschenes *et al.* (1996). Some axons entered STN from the ventral border, and these were often collaterals of axons that innervate further caudal structures including the red nucleus and the deep mesencephalic nucleus. LV-labeled axons in STN were thin and bore both en passant and pedunculated boutons (Fig. 5C).

EM examination of 104 CM+Pf synaptic boutons in STN was performed. Eighty of 104 boutons synapsed on dendritic shafts with the shortest diameters ranging 0.13–1.48 μm (mean ± SD; 0.63 ± 0.30), and 24 synapsed on spines with the shortest diameters averaging 0.30 ± 0.11 μm (Fig. 6). Figure 6D shows that CM+Pf axons synapse on slightly smaller dendrites than randomly sampled asymmetric synapses (data from Chang *et al.*, 1983), however the difference was insignificant. The morphological features of synaptic boutons forming synapses on dendrites and spines were very similar. The size of the boutons was 0.80 ± 0.24 and 0.49 ± 0.13 μm in the longest and shortest diameters, respectively. The boutons contained round vesicles and made asymmetrical synaptic contact with the length of the active zone of 0.28 ± 0.10 μm (Fig. 6).

LV injections in SC were performed in six rats. LV injection in the lateral part of SC resulted in moderate to dense labeling of axons and boutons in the ventral part of ZIv, the Forel field H2, and moderate labeling in a thin part of the dorsolateral STN adjacent to ZIv. Moderate labeling of axons was also observed in ZId and sparse labeling in the medial part of STN and adjacent LHA (Figs 4C and 5). LV injection in the mid-mediolateral part of SC resulted in a similar distribution pattern of labeled-axons in the subthalamus with slightly less dense labeling compared to the LV injections in the lateral part of SC (Fig. 4D). LV injection in the medial part of SC resulted in very sparse labeling in ZI and STN (Figure not shown). The results of FG and LV tracing show that a thin dorsolateral part of STN receives moderate projection and the ventromedial part of STN and adjacent LHA receive sparse projections from the lateral part of SC.

The ZI, the Forel field H2, and the dorsolateral part of STN were innervated by SC axons arriving from multiple directions. Most of the axons traveled from SC in an anterolateral direction through the lateral posterior thalamic nucleus, then rostroventrally through either the lateral or medial side of the medial geniculate nucleus, and then entered the lateral part of ZI and traveled in both rostral and medial directions within ZI. Another group of axons diffusely spread and traveled in the rostroventral direction through the deep mesencephalic nucleus and the rostrally adjacent thalamic reticular area, traveled across the medial lemniscus and the superior cerebella peduncle, and then entered ZId. The labeled-axons in the subthalamus were thin and bore both en passant and pedunculated boutons (Fig. 5F).

Discussion

This study revealed that the areas similar to CM and Pf of the primate could be recognized in the rat. The Pf-like area sends heavy topographically organized projection to the entire STN but very

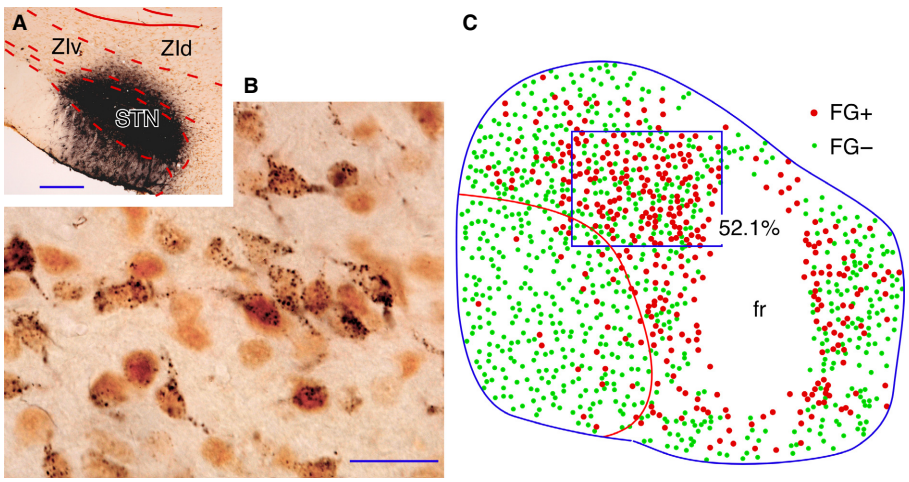

FIG. 3. (A and B) Photomicrograph of an FG and NeuN immunostained section shows FG injection in STN (A) and FG+/NeuN+ and FG-/NeuN+ neurons in CM+Pf. (C) A drawing of FG+ and FG- neurons in CM+Pf. The ventrolateral part of the CM+Pf, marked by a red line, is noticeably sparse with neurons and has only occasional FG+ neurons compared to the dorsomedial CM+Pf, in which 52.1% of neurons are FG+. The scale bar in A is 0.5 mm and in B, 50 μm. [Color figure can be viewed at wileyonlinelibrary.com].

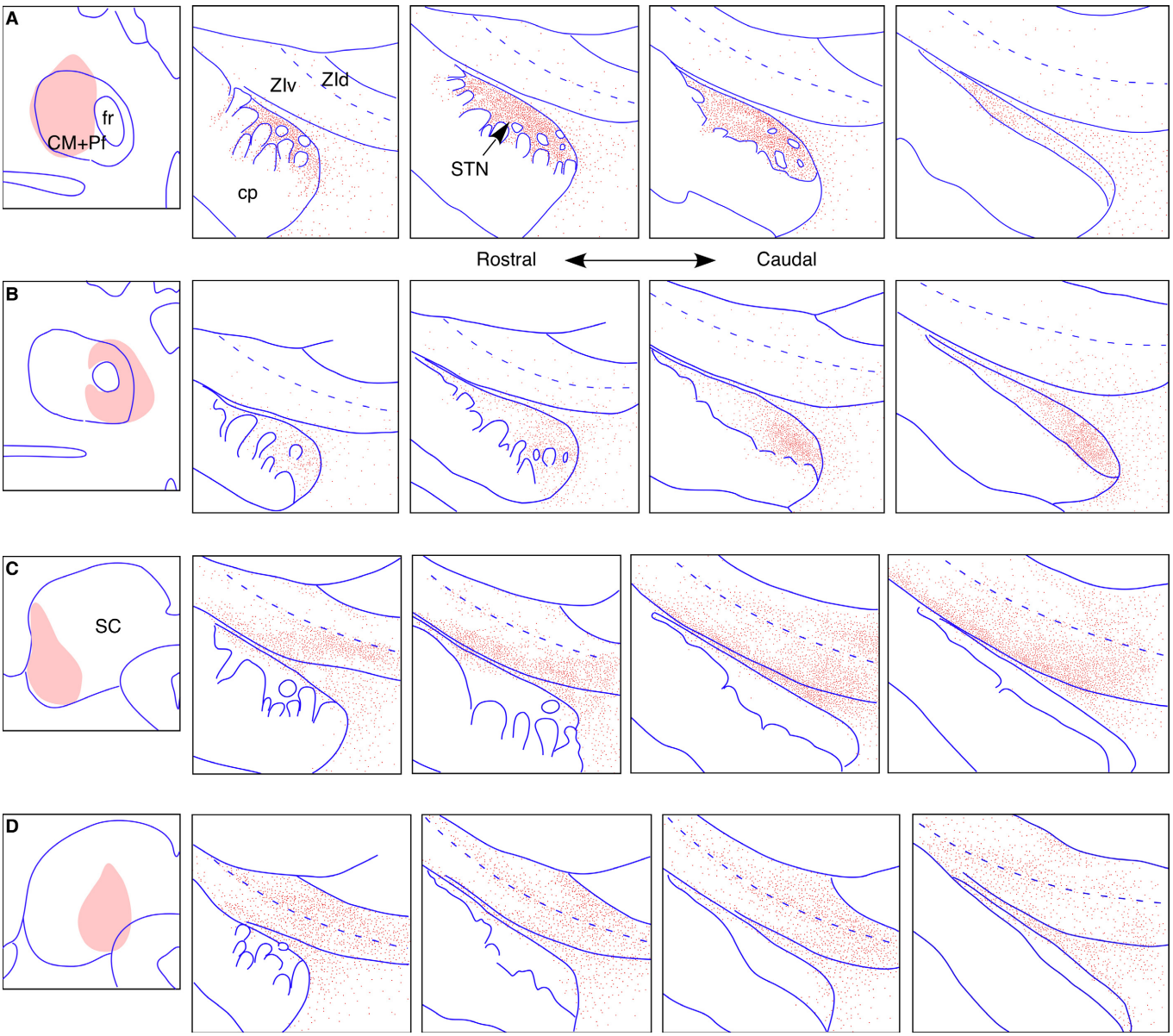

FIG. 4. Drawings of sections show the distributions of LV-labeled boutons in the subthalamus after LV injections into the CM+Pf (A and B) and SC (C and D). [Color figure can be viewed at wileyonlinelibrary.com].

sparse projection to ZI, which suggests that Pf might effectively control basal ganglia function through STN. The projection from CM-like area to the subthalamus was very sparse. The lateral part of the deep layers of SC sends very heavy projection to ZI and moderate to sparse projection to limited parts of STN, suggesting that SC is involved in a limited control of basal ganglia function. Together with other known anatomical connections and physiological data, the possible functionality of the intralaminar and tectal connections to the subthalamus is discussed below.

Identification of CM and Pf

We used FoxP2 immunostaining to identify STN and CM+Pf, as these nuclei contain abundant FoxP2+ neurons (Campbell *et al.*, 2009; Reimers-Kipping *et al.*, 2011). Indeed, we found that more than 90% of the neurons in STN and CM+Pf were FoxP2+ (Kita and Kita, unpublished data).

Although the designation Pf has often been used for rodent posterior intralaminar nuclei in recent publications, early investigators considered the lateral part of CM+Pf in the rodent as homologous to CM in the primate (e.g., Kuhlenbeck, 1954; Albe-Fessard *et al.*, 1966). Some neurotracing studies on the thalamo-striatal projections also suggested that a CM equivalent exists in rodent CM+Pf (Groenewegen & Berendse, 1994; Galvan & Smith, 2011) because the CM equivalent projected mainly to the sensorimotor territory of the striatum similarly to the projections in the cat and the monkey. In this study on rat brain sections, the use of NeuN and FoxP2 immunostaining methods, which visualize neurons and nuclei much more clearly than Nissl staining, revealed very cell dense dorsolateral and medial parts and a less dense ventrolateral part of CM+Pf. Our previous anterograde tracing study in rats revealed that the ventrolateral part of CM+Pf projects to the sensorimotor and association territories of the striatum and that dorsolateral and medial Pf project to the sensorimotor and association/limbic territories of the striatum,

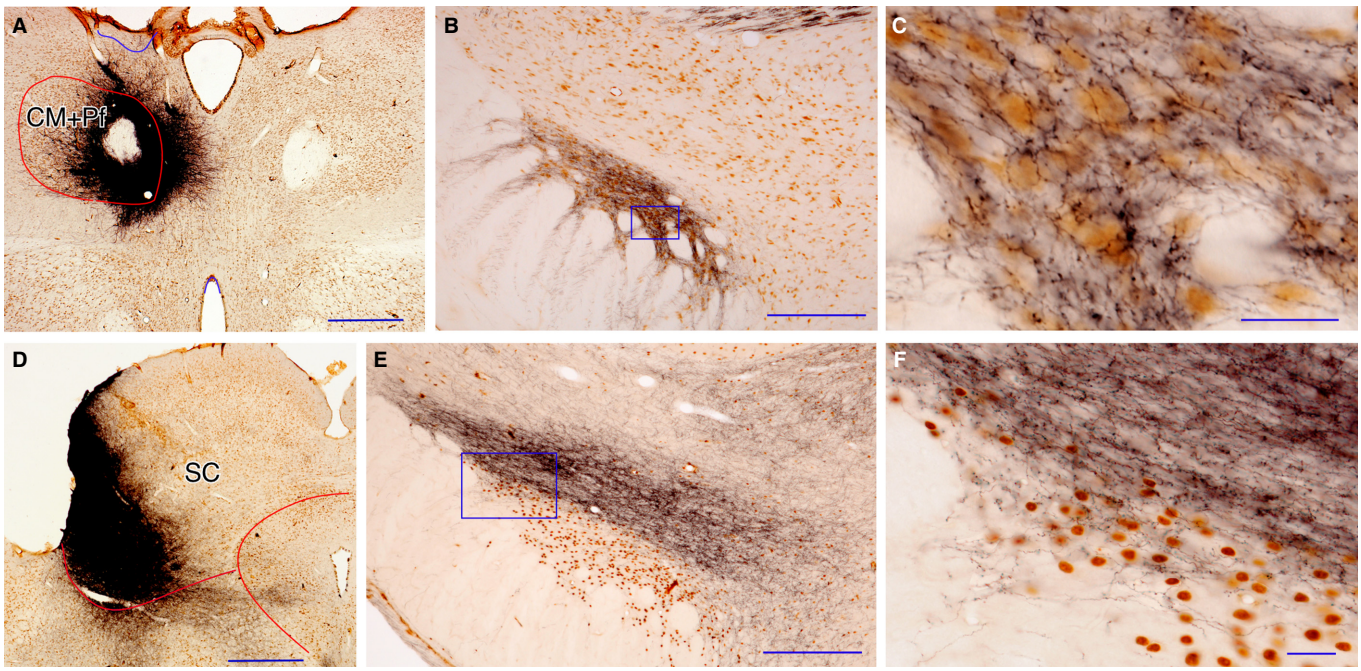

FIG. 5. Photomicrographs show LV injection sites and LV-labeled axons and boutons in the subthalamus after LV injection in the lateral part of CM+Pf (A–C) and in the deep layers in the lateral part of SC (D–F). (C and F) Higher magnification view of the boxed area in (B and E). The section in (A–D) are immunostained for EYFP and NeuN and the section in (E and F) for EYFP and FoxP2. FoxP2+ neurons are in STN but not in H2 or ZI, which indicates that EYFP-labeled SC axons innervate the dorsolateral part of STN. The scale bars in (A and C) are 1.0 mm in (B and E) are 0.5 mm and in (C and F) are 50 μm. [Color figure can be viewed at wileyonlinelibrary.com].

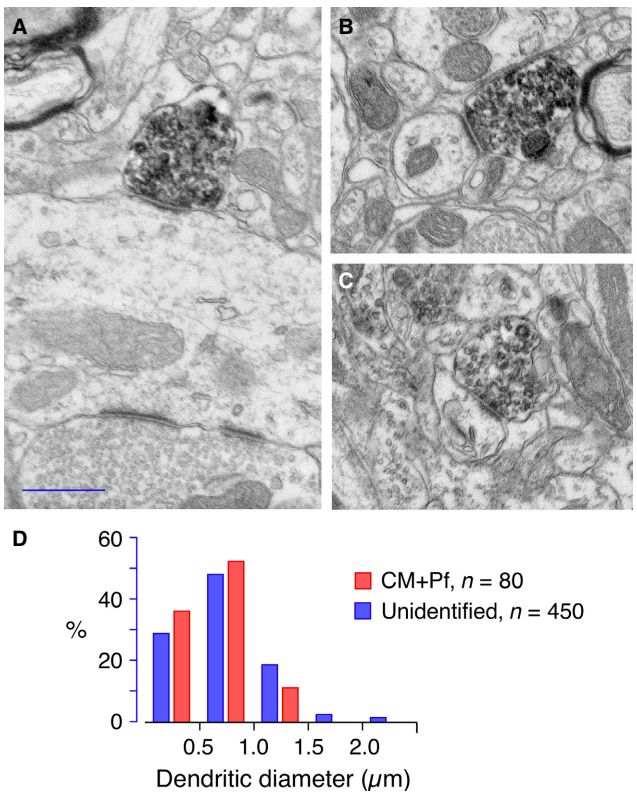

FIG. 6. (A–C) Electron micrographs show examples of EYFP-labeled CM+Pf boutons on a large dendrite (A), a small dendrite (B), and a spine (C) in STN. The scale bar is 500 nm. (D) Distributions of CM+Pf boutons and boutons forming asymmetric synapses observed in unstained sections (i.e., unidentified) on dendrites of STN neurons. The data on unidentified boutons are from Chang *et al.* (1983). [Color figure can be viewed at wileyonlinelibrary.com].

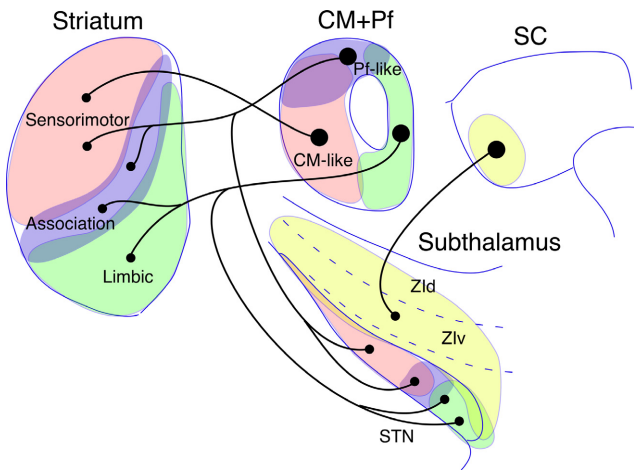

FIG. 7. A diagram of CM+Pf and the SC projection pattern to the striatum and the subthalamus. [Color figure can be viewed at wileyonlinelibrary.com].

respectively (Fig. 7; Yasukawa *et al.*, 2004). We have re-confirmed these CM+Pf projections to the striatum using the FG retrograde tracing method (Kita and Kita, unpublished observation). The similarities of the posterior intralaminar nuclei among the different species described above clearly indicate that the rat CM+Pf indeed consists of recognizable CM and Pf parts, similar to cat and monkeys.

CM+ Pf and Eth projection to STN

We estimated that approximately 50% of neurons in the dorsolateral and medial CM+Pf project to STN. Conversely, very few neurons in

the ventrolateral part of CM+Pf project to STN, which is similar to the observation in monkeys that CM sends a very sparse projection to STN (Sadikot *et al.*, 1992). A single neuron tracing study in rats reported that approximately 20% of the axons of lateral CM+Pf neurons innervating the striatum and the cortex emitted collaterals innervating STN (Deschenes *et al.*, 1996). The difference in the numbers may be attributed to the difference in sampling areas, since only a very small number of neurons in the ventrolateral part of CM+Pf project to STN, as described above.

LV injections in CM+Pf resulted in very dense labeling of axons and boutons in STN and moderate labeling in the lateral part of LHA. The latter receives inputs from the limbic parts of the basal ganglia including the limbic territory of the striatum and the ventral pallidum (Groenewegen & Berendse, 1990). LV injections in CM+Pf resulted in very sparse labeling in ZI. Thus the present results showed that CM+Pf densely and exclusively innervates to basal ganglia related structures. Previous results using biotinylated dextran amine (BDA) or Phaseolus vulgaris-leucoagglutinin (PHA-L) methods implied that CM+Pf projects to both STN and ZIv (Sugimoto *et al.*, 1983; Groenewegen & Berendse, 1990; Bevan *et al.*, 1995). We believe the differences are due to the LV method, which is superior for labeling fine axons and do not label axons passing through the injection site.

We found that FG injections to STN labeled many Eth neurons. Eth is considered a member of the posterior intralaminar nuclei because it projects to the striatum (Parent & De Bellefeuille, 1983; Hu & Jayaraman, 1986; Deschenes *et al.*, 1996). Deschenes *et al.* (1996) further showed that the somato-dendritic morphological features of Eth neurons are very similar to those of CM+Pf neurons and that their axons projecting to the striatum and the cerebral cortex emit collaterals innervating both segments of the globus pallidus. Our study contributes additional insight that many of these neurons are FoxP2+ and there axons extend collaterals to STN.

Topography of CM+ Pf projection to STN

CM+Pf projection to STN showed a mediolateral and rostrocaudal parallel topography as reported by Bevan *et al.* (1995). There were slight differences from other reports in the rat (e.g., Sugimoto *et al.*, 1983; Groenewegen & Berendse, 1990), which may be due to the differences in the tracer injection sites, as Bevan *et al.* (1995) discussed. The present results revealed differences in the functional territorial organization between the rat and the monkey. In the rat, the dorsolateral part of CM+Pf, which projects to the striatal sensorimotor and association territories, projects heavily to the lateral and middle parts of STN. The medial part of CM+Pf, which projects to the striatal association/limbic territories, projects heavily to the medial 2/3 of STN and adjacent LHA (Fig. 7). Thus, the entire STN is covered with heavy projection from CM+Pf. In the monkey, Sadikot *et al.* (1992) found using the PHA-L method that the middle to lateral sensorimotor territory of STN receives very sparse projection from CM and the medial association and limbic territories of STN receive moderate projection from Pf. Thus, unlike the rat, the lateral half of monkey STN receives sparse projection from CM+Pf. A single axon tracing study using the BDA method in the monkey did not find any CM+PF neurons sending collaterals to STN (Parent & Parent, 2005), which implies that the number of neurons projecting to STN may be very small in the primate. The differences described above probably reflect species differences in that the rodent lacks a large frontal association cortex and its associated projection areas in the striatum and STN and/or that CM+Pf to STN projections in the rodent have heavier roles in controlling the activity of STN neurons. Another possibility is that the PHA-L and BDA methods used in the monkey studies were unable to reveal the entire extent of fine collateral axons in STN.

Synaptic sites

The present EM study confirmed a previous study that CM+Pf axons form synapses on dendrites and spines of STN neurons (Bevan *et al.*, 1995). The distribution of the diameter of dendrites suggested that postsynaptic sites are secondary or more distal dendritic shafts (Kita *et al.*, 1983). The comparison of the diameter of post synaptic dendrites suggested that CM+Pf axons synapse on similar size of dendrites to randomly sampled asymmetric synapses, which included those formed by local collateral axons of STN neurons, cortical, thalamic, and pedunculopontine axons (data from Chang *et al.*, 1983).

Functional implications of CM+ Pf projection to STN

Kimura's group found that monkey CM+Pf neurons responded to a wide variety of sensory stimuli, including somatic, visual, and auditory, that were behaviorally relevant and that the pattern of responses in CM and Pf differ significantly. Neurons in Pf responded predominantly with a short-latency facilitation, and were therefore named the SLF type, and those in CM with a long-latency facilitation (LLF), with some LLF preceded by a short-latency suppression (Matsumoto *et al.*, 2001; Minamimoto *et al.*, 2005). In their behavioral choice experiments, SLF neurons responded very strongly to cue and to invalidly cued target visual stimuli, which would evoke attentional orienting in monkeys. In contrast, LLF neurons showed a short-latency suppression after cue and subsequent increase after cue/or target stimuli.

Although both SLF and LLF neurons might be involved in evoking attentional orienting in the monkey, the differences in the response patterns and anatomical connections between CM and Pf suggest involvement in different functional roles. The anatomical connections discussed above suggest that CM may control basal ganglia activity mainly through the sensorimotor territories of the striatum and the globus pallidus, whereas Pf controls through the association and limbic territories of the striatum, the globus pallidus, and STN. Recent studies revealed that intralaminar projection to the striatum can control activity of striatal projection neurons and cholinergic interneurons (Ding *et al.*, 2010; Ellender *et al.*, 2013; Alloway *et al.*, 2014). The physiological features of the intralaminar projections to the pallidum are unknown. Electrical stimulation of CM+Pf evoked a short latency strong excitation in STN neurons in the rat (Mouroux *et al.*, 1995). The present anatomical results are consistent with the strong CM+Pf to STN excitation. STN neurons in the rat and the monkey responded to attentional visual, auditory, and somatic stimuli with the latency consistent with excitation driven by SLF in Pf (Matsumura *et al.*, 1992; Cheruel *et al.*, 1996; Sieger *et al.*, 2015). Activation of STN can evoke very short latency excitation in the basal ganglia output nuclei, the globus pallidus internal segment (GPi) and the substantia nigra pars reticulata (SNr), while striatum-GPi/SNr are slow inhibitory connections (Kita *et al.*, 1983). Thus, behaviorally relevant SLF can reach the basal ganglia output nuclei more quickly through the Pf-STN-GPi/SNr pathway than via the CM+Pf-striatum-GPi/SNr pathway. The functional topographical organization of the CM+Pf-striato-GPi/SNr pathway is better segregated than that of the highly overlapped Pf-STN-GPi/SNr pathway. These anatomical and physiological data imply that the Pf-STN-GPi/SNr and CM+Pf-striatum-GPi/SNr pathways play different

roles. If the CM+Pf-striatum-GPi/SNr pathway is involved in generating attentionally oriented behavior (Matsumoto *et al.*, 2001; Minamimoto *et al.*, 2005; Ding *et al.*, 2010), and if the monosynaptic cortico-STN pathway acts as a brake on execution following conflict or errors by increasing the decision threshold (Frank, 2006; Cavanagh *et al.*, 2011; Ratcliff & Frank, 2012), it is conceivable that the Pf-STN-GPi/SNr pathway is involved in the generation of a very fast internal braking mechanism to prevent or suppress attentional stimulus-invoked panic actions. Another hypothesis is that the pathway may drive preparatory baseline elevation of GPi/SNr activity before the striatum-mediated selected action signal arrives, which may provide higher accuracy behavior with slowed reaction times (Zaghloul *et al.*, 2012).

SC projection to the subthalamus

The SC projection to ZI has been well documented (Roger & Cadusseau, 1985; Shammah-Lagnado *et al.*, 1985; Kolmac *et al.*, 1998; Tokuno *et al.*, 1994; Mitrofanis, 2005; Watson *et al.*, 2015). The main controversy regarding the tectal projection to the subthalamus is whether the main projection sites of SC include STN. Our results showed that the rostrolateral part of the deep layers of SC projects heavily to ZIv and moderately to ZId. The lateral part of SC also projects moderately to the very thin limited area of the dorsolateral STN, which is ventrally adjacent to ZIv, and very sparsely to the medial part of STN. The SC-projecting area of the dorsolateral STN receives projections from the visual cortex (Kita *et al.*, 2014), suggesting the possible convergence of SC and visual cortex mediated visual signals in this area. The STN projection was sparse from the middle to medial parts of SC. The SC projection to STN that we observed was resembled to that reported by Coizet *et al.* (2009), although we confirmed other studies that the main SC projection site in the subthalamus is ZI (Roger & Cadusseau, 1985; Shammah-Lagnado *et al.*, 1985; Tokuno *et al.*, 1994; Kolmac *et al.*, 1998; Watson *et al.*, 2015). It is likely that the reasons for the inconsistency in previous reports were due to the differences in the tracer injection sites and tracers used.

Author contributions

HK designed research. TK, NS, and HK performed research and analyzed data. TK, NS, and HK wrote the paper.

Conflict of interest

The authors declare no conflicts of interest.

Acknowledgements

This work was supported by the National Institute of Neurological Disorders and Stroke Grant NS-57236 (HK and TK) and JSPS Institutional Program for Young Researcher Overseas Visits (NS). We thank R. Kita for editing the manuscript.

Abbreviations

APT, Anterior pretectal nucleus; CL, Centrolateral thalamic nucleus; CM, Centromedian thalamic nucleus; Eth, Ethmoid thalamic nucleus; EYFP, Enhanced yellow fluorescent protein; FG, Fluoro-Gold; FoxP2, Forkhead box protein P2; fr, Fasciculus retroflexus; GPi, Globus pallidus internal segment; H2, Forel field H2; LHA, Lateral hypothalamic area; LHb, Lateral habenular nucleus; LLF, Long-latency facilitation; LV, Lentiviruses; MD, Mediodorsal thalamic nucleus; NeuN, Neuron-specific nuclear protein; PAG, Periaqueductal gray; Pf, Parafascicular nuclei; Po, Posterior thalamic nuclear group; PV, Parvalbumin; PVG, Periventricular gray; SC, Superior colliculus; SLF, Short-latency facilitation; SNr, Substantia nigra pars reticulata; SPFPC, Subparafascicular thalamic nucleus, parvicellular part; STN, Subthalamic nucleus; ZI, Zona incerta; ZId, Dorsal zona incerta; ZIv, Ventral zona incerta.

References

Albe-Fessard, D., Stutinsky, F. & Libouban, S. (1966) *Atlas Stéréotaxique du Diencéphale du Rat Blanc*. Éditions du Centre National de la Recherche Scientifique, Paris.

Alloway, K.D., Smith, J.B. & Watson, G.D. (2014) Thalamostriatal projections from the medial posterior and parafascicular nuclei have distinct topographic and physiologic properties. *J. Neurophysiol.*, **111**, 36–50.

Bevan, M.D. & Bolam, J.P. (1995) Cholinergic, GABAergic, and glutamate-enriched inputs from the mesopontine tegmentum to the subthalamic nucleus in the rat. *J. Neurosci.*, **15**, 7105–7120.

Bevan, M.D., Francis, C.M. & Bolam, J.P. (1995) The glutamate-enriched cortical and thalamic input to neurons in the subthalamic nucleus of the rat: convergence with GABA-positive terminals. *J. Comp. Neurol.*, **361**, 491–511.

Campbell, P., Reep, R.L., Stoll, M.L., Ophir, A.G. & Phelps, S.M. (2009) Conservation and diversity of Foxp2 expression in muroid rodents: functional implications. *J. Comp. Neurol.*, **512**, 84–100.

Cavanagh, J.F., Wiecki, T.V., Cohen, M.X., Figueroa, C.M., Samanta, J., Sherman, S.J. & Frank, M.J. (2011) Subthalamic nucleus stimulation reverses mediofrontal influence over decision threshold. *Nat. Neurosci.*, **14**, 1462–1467.

Celio, M.R. & Heizmann, C.W. (1981) Calcium-binding protein parvalbumin as a neuronal marker. *Nature*, **293**, 300–302.

Chang, H.T., Kita, H. & Kitai, S.T. (1983) The fine structure of the rat subthalamic nucleus: an electron microscopic study. *J. Comp. Neurol.*, **221**, 113–123.

Cheruel, F., Dormont, J.F. & Farin, D. (1996) Activity of neurons of the subthalamic nucleus in relation to motor performance in the cat. *Exp. Brain Res.*, **108**, 206–220.

Coizet, V., Graham, J.H., Moss, J., Bolam, J.P., Savasta, M., McHaffie, J.G., Redgrave, P. & Overton, P.G. (2009) Short-latency visual input to the subthalamic nucleus is provided by the midbrain superior colliculus. *J. Neurosci.*, **29**, 5701–5709.

Deschenes, M., Bourassa, J., Doan, V.D. & Parent, A. (1996) A single-cell study of the axonal projections arising from the posterior intralaminar thalamic nuclei in the rat. *Eur. J. Neurosci.*, **8**, 329–343.

Ding, J.B., Guzman, J.N., Peterson, J.D., Goldberg, J.A. & Surmeier, D.J. (2010) Thalamic gating of corticostriatal signaling by cholinergic interneurons. *Neuron*, **67**, 294–307.

Ellender, T.J., Harwood, J., Kosillo, P., Capogna, M. & Bolam, J.P. (2013) Heterogeneous properties of central lateral and parafascicular thalamic synapses in the striatum. *J. Physiol.*, **591**, 257–272.

Frank, M.J. (2006) Hold your horses: a dynamic computational role for the subthalamic nucleus in decision making. *Neural Networks*, **19**, 1120–1136.

Galvan, A. & Smith, Y. (2011) The primate thalamostriatal systems: anatomical organization, functional roles and possible involvement in Parkinson's disease. *Basal Ganglia*, **1**, 179–189.

Groenewegen, H.J. & Berendse, H.W. (1990) Connections of the subthalamic nucleus with ventral striatopallidal parts of the basal ganglia in the rat. *J. Comp. Neurol.*, **294**, 607–622.

Groenewegen, H.J. & Berendse, H.W. (1994) The specificity of the 'non-specific' midline and intralaminar thalamic nuclei. *Trends Neurosci.*, **17**, 52–57.

Hu, H. & Jayaraman, A. (1986) The projection pattern of the suprageniculate nucleus to the caudate nucleus in cats. *Brain Res.*, **368**, 201–203.

Kita, H. (1994) Physiology of two disynaptic pathways from the sensorimotor cortex to the basal ganglia output nuclei. In Percheron, G., McKenzie, J.S. & Feger, J. (Eds), *The Basal Ganglia IV*. Plenum, New York, pp. 263–276.

Kita, H. & Kita, T. (2001) Number, origins, and chemical types of rat pallidostriatal projection neurons. *J Comp Neurol*, **437**, 438–448.

Kita, T. & Kita, H. (2011) Cholinergic and non-cholinergic mesopontine tegmental neurons projecting to the subthalamic nucleus in the rat. *Eur. J. Neuorsci.*, **33**, 433–443.

Kita, H., Chang, H.T. & Kitai, S.T. (1983) The morphology of intracellularly labeled rat subthalamic neurons: a light microscopic analysis. *J. Comp. Neurol.*, **215**, 245–257.

Kita, T., Osten, P. & Kita, H. (2014) Rat subthalamic nucleus and zona incerta share extensively overlapped representations of cortical functional territories. *J. Comp. Neurol.*, **522**, 4043–4056.

Kolmac, C.I., Power, B.D. & Mitrofanis, J. (1998) Patterns of connections between zona incerta and brainstem in rats. *J. Comp. Neurol.*, **396**, 544–555.

Kuhlenbeck, H. (1954) Some histologie age changes in the rat's brain and their relationship to comparable changes in the human brain. *Confin. Neurol.*, **14**, 329–342.

Matsumoto, N., Minamimoto, T., Graybiel, A.M. & Kimura, M. (2001) Neurons in the thalamic CM-Pf complex supply striatal neurons with information about behaviorally significant sensory events. *J. Neurophysiol.*, **85**, 960–976.

Matsumura, M., Kojima, J., Gardiner, T.W. & Hikosaka, O. (1992) Visual and oculomotor functions of monkey subthalamic nucleus. *J. Neurophysiol.*, **67**, 1615–1632.

Minamimoto, T., Hori, Y. & Kimura, M. (2005) Complementary process to response bias in the centromedian nucleus of the thalamus. *Science*, **308**, 1798–1801.

Mitrofanis, J. (2005) Some certainty for the "zone of uncertainty"? Exploring the function of the zona incerta. *Neuroscience*, **130**, 1–15.

Mouroux, M. & Feger, J. (1993) Evidence that the parafascicular projection to the subthalamic nucleus is glutamatergic. *Neuroreport*, **4**, 613–615.

Mouroux, M., Hassani, O.K. & Feger, J. (1995) Electrophysiological study of the excitatory parafascicular projection to the subthalamic nucleus and evidence for ipsi- and contralateral controls. *Neuroscience*, **67**, 399–407.

Parent, A. & De Bellefeuille, L. (1983) The pallidointralaminar and pallidonigral projections in primate as studied by retrograde double-labeling method. *Brain Res.*, **278**, 11–27.

Parent, A. & Hazrati, L.N. (1995) Functional anatomy of the basal ganglia. I. The cortico-basal ganglia-thalamo-cortical loop. *Brain Res. Brain Res. Rev.*, **20**, 91–127.

Parent, M. & Parent, A. (2005) Single-axon tracing and three-dimensional reconstruction of centre median-parafascicular thalamic neurons in primates. *J. Comp. Neurol.*, **481**, 127–144.

Ratcliff, R. & Frank, M.J. (2012) Reinforcement-based decision making in corticostriatal circuits: mutual constraints by neurocomputational and diffusion models. *Neural Comput.*, **24**, 1186–1229.

Reimers-Kipping, S., Hevers, W., Paabo, S. & Enard, W. (2011) Humanized Foxp2 specifically affects cortico-basal ganglia circuits. *Neuroscience*, **175**, 75–84.

Roger, M. & Cadusseau, J. (1985) Afferents to the zona incerta in the rat: a combined retrograde and anterograde study. *J. Comp. Neurol.*, **241**, 480–492.

Royce, G.J. & Mourey, R.J. (1985) Efferent connections of the centromedian and parafascicular thalamic nuclei: an autoradiographic investigation in the cat. *J. Comp. Neurol.*, **235**, 277–300.

Sadikot, A.F., Parent, A. & Francois, C. (1992) Efferent connections of the centromedian and parafascicular thalamic nuclei in the squirrel monkey: a PHA-L study of subcortical projections. *J. Comp. Neurol.*, **315**, 137–159.

Shammah-Lagnado, S.J., Negrao, N. & Ricardo, J.A. (1985) Afferent connections of the zona incerta: a horseradish peroxidase study in the rat. *Neuroscience*, **15**, 109–134.

Sieger, T., Serranova, T., Ruzicka, F., Vostatek, P., Wild, J., Stastna, D., Bonnet, C., Novak, D. *et al.* (2015) Distinct populations of neurons respond to emotional valence and arousal in the human subthalamic nucleus. *Proc. Natl. Acad. Sci. USA*, **112**, 3116–3121.

Smith, Y., Galvan, A., Raju, D. & Wichmann, T. (2010) "Anatomical and Functional organization of the thalamostriatal systems." In Steiner, H. & Tseng, K.Y. (Eds), *Handbook of Basal Ganglia Structure and Function: A Decade of Progress*. Elsevier, New York, NY, pp. 381–392.

Smith, Y., Galvan, A., Ellender, T.J., Doig, N., Villalba, R.M., Huerta-Ocampo, I., Wichmann, T. & Bolam, J.P. (2014) The thalamostriatal system in normal and diseased states. *Front. Syst. Neurosci.*, **8**, 5.

Sugimoto, T., Hattori, T., Mizuno, N., Itoh, K. & Sato, M. (1983) Direct projections from the centre median-parafascicular complex to the subthalamic nucleus in the cat and rat. *J. Comp. Neurol.*, **214**, 209–216.

Tokuno, H., Takada, M., Ikai, Y. & Mizuno, N. (1994) Direct projections from the deep layers of the superior colliculus to the subthalamic nucleus in the rat. *Brain Res.*, **639**, 156–160.

Watson, G.D., Smith, J.B. & Alloway, K.D. (2015) The zona incerta regulates communication between the superior colliculus and the posteromedial thalamus: implications for thalamic interactions with the dorsolateral striatum. *J. Neurosci.*, **35**, 9463–9476.

Yasukawa, T., Kita, T., Xue, Y. & Kita, H. (2004) Rat intralaminar thalamic nuclei projections to the globus pallidus: a biotinylated dextran amine anterograde tracing study. *J. Comp. Neurol.*, **471**, 153–167.

Zaghloul, K.A., Weidemann, C.T., Lega, B.C., Jaggi, J.L., Baltuch, G.H. & Kahana, M.J. (2012) Neuronal activity in the human subthalamic nucleus encodes decision conflict during action selection. *J. Neurosci.*, **32**, 2453–2460.